Binding of Ionic Ligands to Polyelectrolytes*

Dirk Stigter and Ken A. Dill

Department of Pharmaceutical Chemistry, University of California, San Francisco, California 94143 USA

ABSTRACT   Ionic ligands can bind to polyelectrolytes such as DNA or charged polysaccharides. We develop a Poisson-Boltzmann treatment to compute binding constants as a function of ligand charge and salt concentration in the limit of low ligand concentration. For flexible chain ligands, such as oligopeptides, we treat their conformations using lattice statistics. The theory predicts the salt dependence and binding free energies, of Mg^{2+} ions to polynucleotides, of hexamine cobalt(III) to calf thymus DNA, of polyamines to T7 DNA, of oligolysines to poly(U) and poly(A), and of tripeptides to heparin, a charged polysaccharide. One parameter is required to obtain absolute binding constants, the distance of closest separation of the ligand to the polyion. Some, but not all, of the binding entropies and enthalpies are also predicted accurately by the model.

INTRODUCTION

We consider the binding of charged ligands to polyelectrolytes in monovalent salt solutions. The strength of binding of ligands such as proteins and other multivalent ions to DNA often depends strongly on the supporting salt concentration (Latt and Sober, 1967; Riggs et al., 1970a,b; Record et al., 1976; Plum and Bloomfield, 1988; Mascotti and Lohman, 1990). This indicates the importance of interionic interactions. Manning (1978) has applied his counterion condensation theory to the binding of multivalent ions to polyelectrolytes. Wilson et al. (1980) used a Poisson-Boltzmann model for the polyelectrolyte. They found that predictions are not very different from those of Manning's approach, in fair agreement for the binding of Mg^{2+} and spermidine^{3+} to double-stranded DNA. Other previous work treats the slope of binding versus salt, $\partial \log K_{obs}/\partial \log M_{salt}$, but not the actual binding constant K_{obs} itself. These treatments range from counterion condensation and thermodynamic theories (Record et al., 1976; Manning, 1978; Friedman and Manning, 1984; Anderson and Record, 1982, 1993) to the more detailed structural modeling of protein-DNA and antibiotic-DNA complexes using the nonlinear Poisson-Boltzmann (PB) equation (Misra et al., 1994a,b). In our work, we treat the binding equilibrium using the PB theory instead of the counterion condensation model, based on our view that PB is a more accurate model of electrostatics (Stigter, 1995), starting from Mayer cluster integrals for binary interactions. We do not treat the structural detail, as is done in finite difference PB methods (Misra et al., 1994a,b). We find that the theory agrees well with experiments on the binding to B-DNA, single-stranded polynucleotides and heparin of small ions such as Mg^{2+} and

Co $(NH_3)_6^{3+}$ and of larger ions such as oligolysines and polyamines.

Fig. 1 indicates the process of interest here, of binding ligand L to polynucleotide P to form a bound complex B:

$$P + L \rightarrow B \qquad (1)$$

The measured binding constant is defined as $K_{obs} = [B]/[L][P]$ where $[L]$ is the concentration (molarity) of free ligand, $[P]$ is the concentration of free binding sites (nucleotides) on the DNA, and $[B]$ is the concentration of the bound complex. This binding constant K_{obs} may depend on salt concentration. It is standard practice to extrapolate K_{obs} to infinite dilution of ligand concentration, and to determine the dependence on salt concentration, $\partial \log K_{obs}/\partial \log M_{salt}$. Fig. 2 shows experimental results of Mascotti and Lohman (1990) for the binding of oligolysines, with $z = 2$ to 10 charges per ion, to poly(U) as a function of salt concentration. Table 1 gives the slopes of the straight lines in fig 2, $\partial \log K_{obs}/\partial \log M_{salt}$, and the intercepts. In the next section we develop microscopic theory in which the binding is given by the pair cluster integral for the interaction between a polyion and a ligand ion. For cases in which the ligand itself is a chain molecule, we treat the conformational and charge distributions using a polymer lattice model.

Fig. 1 shows the equilibrium binding of a z-valent ion L^{z+} with solution concentration $[L]$ to a sequence of z negatively charged sites on a polyion with concentration $[P]$ to form a complex B. We treat the association as an ion exchange reaction that formally releases z K^+ counterions from the polyion P and z Cl^- counterions from the ligand L to the bulk solution having salt concentration $[KCl]$. The starting point of the theory is that ligand ions assume a Boltzmann distribution in the electrostatic field around the polyelectrolyte, just as the salt ions do. Binding is then defined in terms of the excess amount of ligand near the polyion compared with the bulk ligand concentration. In the zero binding limit of small multivalent ionic ligands such as Co $(NH_3)_6^{3+}$ this approach requires only the electrostatic PB field around the polyelectrolyte in the supporting monovalent salt solution. In the case of polymeric ligands, such as oligolysines, we
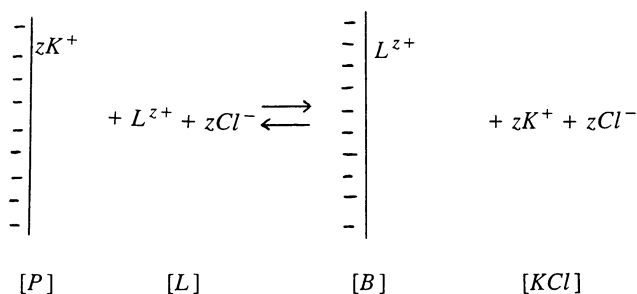
FIGURE 1   Complex formation between z-valent ligand and polyelectrolyte.

FIGURE 2   Binding constants versus monovalent salt concentration for binding of oligolysines to poly(U). Numbers indicate ligand charge z. From Mascotti and Lohman (1990).

must also account for the conformational entropy change of the ligand ion upon binding.

BINDING THEORY

We model the polyelectrolyte as a cylinder with a radius a Å, and a uniform surface charge corresponding to one negative charge e per b Å in length, in a monovalent salt solution. We neglect end effects, so the electrostatic potential ψ around the cylinder has radial symmetry. The electrostatic field $\psi(r)$ is obtained by integrating the PB equation using the method of Stigter (1975). We consider only the cases of high ligand dilution. Hence the PB theory should be applicable to the binding of multivalent ligand ions, even though the PB theory is generally not a good approximation if all counterions are multivalent. Because the ligand is dilute, we can assume the electrostatic potential field ψ is unperturbed by the presence of ligand ions which are treated as point charges, as are the small ions. Extensive data of Mascotti and Lohman (1992) show that ligand binding is not significantly dependent on the nature of the cations or anions of the supporting electrolyte, except for valency effects. This justifies the use of a nonspecific model such as the PB equation.

Computing binding constants from cluster integrals

What is the meaning of binding, and how should we compute a binding constant for a charged ligand to a polyelectrolyte? Because electrostatic interactions are long-ranged, at what distance from the polyion should a ligand be considered to be "bound?" Experimentally, binding constants are determined from the ligand concentration in a polyelectrolyte compartment that is separated by a membrane from a multicomponent solvent. Let us consider a solution consisting of water (component w), polyelectrolyte such as K−DNA (p), monovalent supporting salt KCl (s), and ligand LCl_z (l). The polyions cannot pass the membrane, so in the solvent compartment we have only components w, s, and l. In the notation of Fig. 1 the concentrations in the solution compartment are $c_p = [P]$, $c_s = $ [KCl]. In the solvent compartment concentrations are denoted c_i^*, i.e., c_s^* for KCl and $c_l^* = [L]$ for the free ligand. The difference in
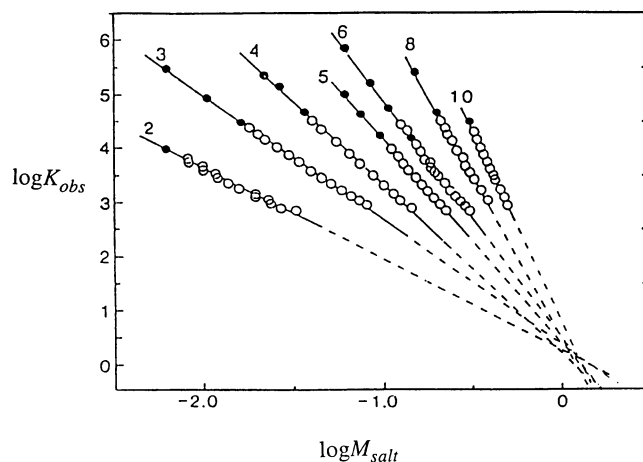
ligand concentration between the compartments, $c_1 - c_1^* = [B]$ gives the binding constant

$$K_{obs} = \frac{[B]}{[L][P]} = \frac{c_1 - c_1^*}{c_1^* c_p} \qquad (2)$$

How do we compute this quantity from theory? As defined in Eq. 2, K_{obs} is the preferential interaction coefficient between polyelectrolyte and ligand. Such interaction coefficients have an exact interpretation in terms of statistical mechanical cluster integrals. This interpretation is based on the work by McMillan and Mayer (1945) who applied the pressure virial expansion of nonideal gases to the osmotic pressure in solution/solvent membrane equilibria, and developed the virial coefficients as cluster integrals. Hill (1958) extended this approach with the cluster integral expansion for the distribution of an equilibrium component in multicomponent membrane equilibria. Stigter and Hill (1959) applied the results to the salt distribution in a Donnan membrane equilibrium such as is considered here, but without ligand component l, and with colloidal spheres as polyions. These differences, however, do not change the formalism. The appropriate virial expansion for the ligand

TABLE 1   Experimental binding data of z-valent oligolysines to poly(U): intercept at 1 M salt and slope of logK_{obs} versus logM_{salt}

z	Intercept*	Slope*	Slope[#]
2	0.26 ± 0.24	−1.68 ± 0.20	−1.75
3	0.36 ± 0.24	−2.30 ± 0.19	−2.54
4	0.20 ± 0.22	−3.10 ± 0.21	−3.17
5	0.37 ± 0.22	−3.76 ± 0.22	−3.65
6	0.49 ± 0.22	−4.36 ± 0.22	−4.18
8	0.46 ± 0.24	−5.95 ± 0.25	−4.98
10	0.77 ± 0.27	−7.02 ± 0.34	−5.47

*Mascotti and Lohman (1990).
[#]From Fig. 7, dashed lines.

distribution between the compartments is

$$\frac{c_1}{c_1^*} = 1 + Ac_p + \cdots \quad T, \mu_w, \mu_s, \mu_l \text{ constant} \quad (3)$$

when the ligand, salt, and solvent components exchange freely through the membrane and have fixed activity in the solvent and solution compartments. The virial coefficient A in Eq. 3 depends on the potential of mean force W between one polyion and one z-valent ligand ion in the limit $c_p \to 0$ (in solvent):

$$A = C \int_V (e^{-W/kT} - 1) dV \quad (4)$$

The constant C in Eq. 4 depends on the units of V and of the concentrations in Eq. 3. Comparing Eqs. 2 and 3 shows that $K_{obs} = A$, so to compute binding constants we must obtain A through use of Eq. 4. Although the binary cluster integral for $K_{obs} = A$ in Eq. 4 is exact, approximations enter when we specify the domain of integration, and when we use the PB theory to obtain the local electrostatic potential ψ in $W = -ze\psi$.

We derive the constant C in Eq. 4 by first considering the bound ligand $[L]K_{obs} = [B]/[P]$ in mol of complex, B, per mol nucleotide, P, or in number of bound L^{z+} ions per binding site. Because the cylinder has radius a Å and the length per binding site is b Å, we have

$$\frac{[B]}{[P]} = [L]N_{Av}10^{-27}I_1 \quad (5)$$

$$I_1 = \left[b \int_a^\infty (e^{z\phi} - 1) 2\pi r \, dr \right] - \pi a^2 b \quad (6)$$

where $\phi = |e\psi/kT|$. The factor $N_{Av}10^{-27}$ in Eq. 5 converts the units of $[L]$, mol/l, into number of ligand ions per Å^3, the reciprocal of which are the units of I_1. The integration is over the entire double layer outside the cylinder, with radius r from a to ∞; with $W = \infty$ for $r < a$, the term $\pi a^2 b$ accounts for the volume of the cylinder per binding site. Dividing both sides of Eq. 5 by $[L]$ yields the ligand binding constant

$$K_{obs} = \frac{[B]}{[L][P]} = N_{Av}10^{-27}I_1 \quad (7)$$

The units of K_{obs} are l per mol of binding sites.

The integral in Eq. 6 gives the integrated excess concentration of ligand ions. Hence, it is in the nature of the Poisson-Boltzmann double layer distribution that some small fraction of the ligand ions that are defined as "bound" will not necessarily be spatially close to the polyelectrolyte. This is shown in Fig. 3, which is the standard view of the way in which a polyelectrolyte molecule perturbs the local small ion concentrations in a KCl solution. Compared with the bulk concentration [KCl] there is an excess of K^+ counterions (horizontal shading) and a deficit of Cl^- ions
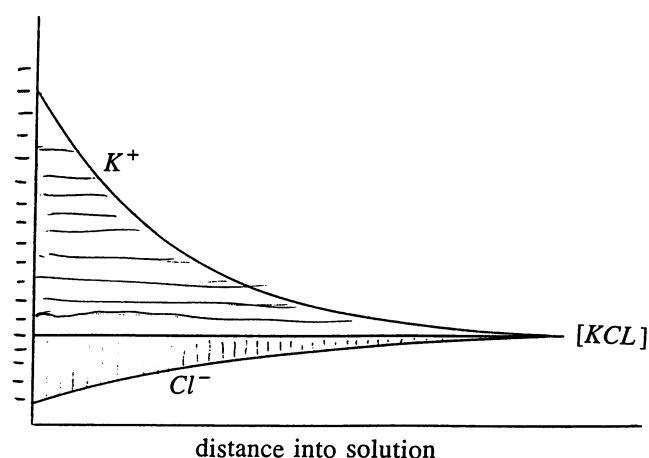

distance into solution

FIGURE 3   Distribution of small ions near negatively charged surface.

(vertical shading), but they neutralize the charge on the polyion only in aggregate when they are integrated over all space. Thus counterion "binding" refers to this enhancement of K^+ concentration integrated over space. The curves in Fig. 3 indicate that the local concentration of K^+ is given by the Boltzmann distribution $[KCl]e^\phi$. Now consider adding a small concentration of the ligand, LCl_z. As with K^+, the concentration of the L^{z+} ions will obey a Boltzmann distribution. The excess concentration of ligand near the polyion (relative to the bulk) is $[L](e^{z\phi} - 1)$, where $[L]$ is the concentration in bulk solution far from the cylinder where $\phi = 0$. The integral over all space of this excess is defined as "bound" ligand in Eqs. 5 and 6.

Binding constants for chain molecule ligands

Now if the charged ligand molecule is a flexible chain instead of a point charge, it introduces additional complexity, for two reasons. First, a flexible ligand will lose conformational entropy on binding. Second, a flexible ligand will have its charge distributed along the chain, and therefore different parts of the ligand will be in different parts of the electrostatic potential field around the polyion. Each charge on the ligand is at a different electrostatic potential. We suppose flexible ligands adopt an ensemble of chain configurations and we compute Boltzmann averages. We treat the electrostatics as before, assuming the polyion is a rod with a uniform surface charge and a PB ionic atmosphere around it. However, now the polyelectrolyte rod is surrounded by a cylindrical lattice containing an ensemble of flexible ligand conformations that are Boltzmann weighted in the PB field around it.

We consider the binding of a linear positively charged polymeric ligand, consisting of n segments, to a negatively charged polyelectrolyte. Some or all of the ligand segments may carry one protonic charge. We compute the conformational ensemble of an isolated bound ligand using the one-dimensional Ising model matrix method, first applied to

polymer adsorption by Rubin (1965), and reviewed by Dill et al. (1988).

A cross-section of the polyion rod and surrounding ligand lattice is shown in Fig. 4. The shaded circle represents the central polyelectrolyte rod with radius a. The salt solution around the rod is divided into concentric layers of lattice cells. Each cell has a volume v_0 and accommodates either one segment of the ligand or else solvent. We assume a pseudo-cubic lattice with a thickness $c = v_0^{1/3}$ for each successive layer, numbered $1, 2, \ldots i, \ldots n$ from the inside out. Because all lattice sites have the same volume, the number of lattice sites in layer i is proportional to the radial distance r_i of the cell centers from the polyelectrolyte axis

$$r_i = a + \left(i - \frac{1}{2}\right)c \tag{8}$$

In general, conformations are built up by starting with the first segment of the ligand molecule in a cell in layer i and propagating the chain, segment by segment, through the lattice, sideways in the same layer, outward from layer i into layer $i + 1$ or, if $i > 1$, inward from layer i into layer $i - 1$. If $z_c = 6$ is the coordination number of the pseudo-cubic cells, each cell in layer i has $z_c - 2$ neighbors in layer i, r_{i+1}/r_i neighbors in layer $i + 1$ and, when $i > 1$, r_{i-1}/r_i neighbors in layer $i - 1$.

We represent the distribution of segment k throughout the layers $i = 1$ to n by the vector

$$v(k) = [v_1(k) \, v_2(k) \cdots v_i(k) \cdots v_n(k)] \tag{9}$$

Each step direction is intrinsically equally probable, if we neglect ligand intrachain excluded volume. Thus, given $v(k)$ by Eq. 9, the distribution for segment $k + 1$ is a conse-

quence of radially outward steps from segment k, $v_{i+1}(k + 1) = (r_{i+1}/r_i)v_i(k)$; lateral steps parallel to the polyion surface, $v_i(k + 1) = (z_c - 2)v_i(k)$; and, for $i > 1$, radially inward steps, $v_{i-1}(k + 1) = (r_{i-1}/r_i)v_i(k)$. Every component of $v(k)$ has a similar propagation relation. But the step directions are biased by local interaction potentials. For example, if segments are held in the first layer by a short range adsorption potential θkT, compared with segments in the bulk solution, the probability of a segment moving into the first layer is multiplied by the Boltzmann factor e^θ. Similarly, for a charged ligand the step of a protonated segment into layer i with electrostatic potential ψ_i is favored by the Boltzmann factor e^{ϕ_i} where $\phi_i = |e\psi_i/kT|$ is the local PB potential in layer i. In sum, $v(k + 1)$ can be generated from $v(k)$ by multiplying $v(k)$ by the $n \times n$ propagation matrix

$$G_n = \begin{bmatrix} (z_c - 2)e^{\phi_1} & \dfrac{r_2}{r_1}e^{\phi_2} & 0 & 0 & \cdot \\[1.5em] \dfrac{r_1}{r_2}e^{\phi_1} & (z_c - 2)e^{\phi_2} & \dfrac{r_3}{r_2}e^{\phi_3} & 0 & \cdot \\[1.5em] 0 & \dfrac{r_2}{r_3}e^{\phi_2} & (z_c - 2)e^{\phi_3} & \dfrac{r_4}{r_3}e^{\phi_4} & \cdot \\[1.5em] 0 & 0 & \dfrac{r_3}{r_4}e^{\phi_3} & (z_c - 2)e^{\phi_4} & \cdot \\[1.5em] \cdot & \cdot & \cdot & \cdot & \cdot \end{bmatrix} \tag{10}$$

In Eq. 10 any short range adsorption potential θ is included in ϕ_1. Taking the relation

$$v(k) = v(k - 1)G_n \tag{11}$$

down to the first segment we find that

$$v(k) = v(1)G_n^{k-1} \tag{12}$$

The matrix G_n can also be used for uncharged chains, for which the electrostatic potentials are $\phi_i = 0$ for all i. Equation 12 gives the distribution function for segment k throughout all the lattice layers as a function of the distribution function of segment 1. For example, if for a charged ligand $v(1) = [e^{\phi_1} \, 0 \, 0 \ldots 0]$, the vector $v(n) = v(1)G_n^{n-1}$ comprises all ligand conformations anchored with the first segment at the surface of the polyelectrolyte, in layer $i = 1$. The total number Z_1 of such adsorbed conformations is the sum of all components of $v(n)$, which is given by the matrix product of $v(n)$ with the n-dimensional unit column vector $u_n = \text{col}[1 \, 1 \ldots 1]$

$$Z_1 = \sum_{i=1}^{n} v_i(n) = v(n) \, u_n = v(1)G_n^{n-1}u_n \tag{13}$$

Z_1 is the canonical partition function of a chain having a distribution $v(1)$ of segment 1.

There are two different types of binding experiments. Because they measure somewhat different properties, they require different theoretical treatment. First, as in the experiments of Mascotti and Lohman (1992, 1993), a fluores
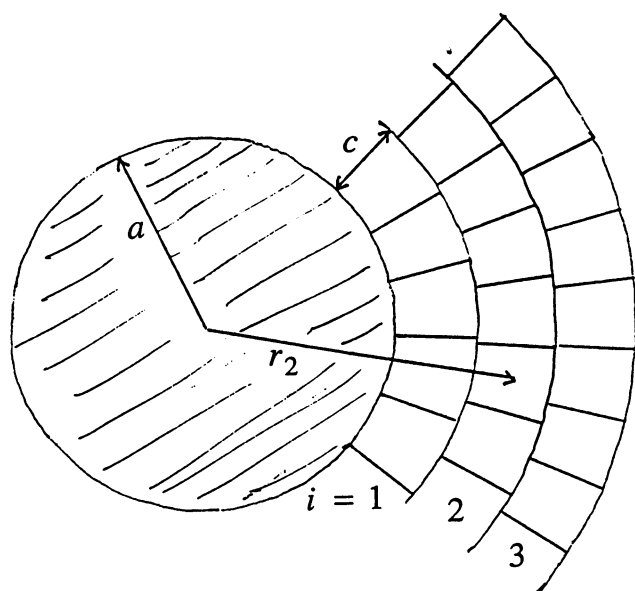

FIGURE 4   Cylindrical lattice for ligand chain conformations around polyelectrolyte rod with radius a (shaded area), with cell layers $i = 1, 2, 3, \ldots n$ of thickness c each and center distance $r_i = r_1, r_2, \ldots$ from axis.

cent probe in the ligand is quenched when it is sufficiently close to the polyion. We call this "localized binding." According to this type of measurement, "binding" refers only to ligands in very close proximity to the polyion. Second, binding may be the excess ligand concentration observed in a membrane experiment as described above. In that case, molecules will also be "bound" that are more distant from the polyion. We call this "delocalized binding." The latter procedure is closely related to Eq. 7 and to the Gibbs definition of adsorption.

Localized binding

Mascotti and Lohman (1990, 1992, 1993) monitored the binding of oligolysines by the fluorescence quenching of tryptophan that was incorporated as the second residue of the ligand chain. To treat this case, we divide a ligand chain into n segments, one for each of the lysines and one for the tryptophan residue. A ligand is considered bound when its tryptophan, the test segment, resides in layer $i = 1$. We treat the partition function of the bound ligand, Z_{bound}, as the product of two components: Z_{short} for segment 1 plus the tryptophan and Z_{long} for the remainder of the chain, given the tryptophan in layer 1.

Table 2 shows the charge distribution on the ligands used by Mascotti and Lohman (1990). The peptides with $z = 2$ and 5 charges have a terminal carboxyl group so the last lysine residue carries no net charge. The other peptides have C-terminal amides. In all cases the first, N-terminal, lysine residue is doubly charged. To determine the influence of the tryptophan marker Mascotti and Lohman (1992) have compared the binding to poly(U) of oligolysines ($z = 6$) containing one, two, and three tryptophan residues. The experiments give approximately $e^{\theta} = 3$ so we use this value in Eq. 14 for Z_{short}. Hence the partition function for the short chain $K^{2+}W$ common to all ligands is

$$Z_{short} = (z_c - 2)e^{2\phi_1 + \theta} + \frac{r_2}{r_1}e^{2\phi_2 + \theta} \qquad (14)$$

where the Boltzmann factor e^{θ} accounts for the tryptophan in layer 1, and the factors $e^{2\phi_1}$ and $e^{2\phi_2}$ account for the doubly charged lysine, K^{2+}, in layer 1 or 2. Table 2 gives expressions for $Z_{bound} = Z_{short}Z_{long}$ for the cases of Mascotti and Lohman given the tryptophan in layer 1, that is,

TABLE 2   Binding of z-valent peptides to poly(U): partition function for bound n monomer ligands

Peptide*	z	n	Partition function Z_{bound}
$K^{2+}WK^{\pm}$	2	3	$Z_{short}\nu(1)\, G_2\, (\phi = 0)\, u_2$
$K^{2+}WK^{+}$	3	3	$Z_{short}\nu(1)\, G_2\, u_2$
$K^{2+}W\,(K^{+})_2$	4	4	$Z_{short}\nu(1)\, G_3^2\, u_3$
$K^{2+}W(K^{+})_3K^{\pm}$	5	6	$Z_{short}\nu(1)\, G_5^3\, G_5(\phi = 0)\, u_5$
$K^{2+}W\,(K^{+})_4$	6	6	$Z_{short}\nu(1)\, G_5^4\, u_5$
$K^{2+}W\,(K^{+})_6$	8	8	$Z_{short}\nu(1)\, G_7^6\, u_7$
$K^{2+}W\,(K^{+})_8$	10	10	$Z_{short}\nu(1)\, G_9^8\, u_9$

*K, lysine; W, tryptophan.

with $\nu(1) = [1\ 0\ \ldots\ 0]$ in Z_{long}. The matrix $G_n(\phi = 0)$ in the expressions for $z = 2$ and 5 accounts for the endchain uncharged segment; it equals the matrix G_n of Eq. 10 with all $\phi_i = 0$. The calculation of the binding constant K_{obs} from Z_{bound} will be given in the next section.

Delocalized binding

Now we apply the same matrix approach to the delocalized binding experiment, where some ligands are considered bound even when they are distant from the polyion. A chain with a protonic charge e on each of its n segments is considered bound whenever it is in excess over the bulk ligand concentration. We compute the total partition function as a sum of components $Z(j)$, which is the number of configurations of a chain having at least one segment in layer j and no segment in earlier layers, 1, 2, 3, ..., $j - 1$. Let us first consider the component $Z(1)$, the number of chain configurations for which at least one of the chain segments is in layer 1. We evaluate $Z(1)$ by further dividing the conformations into subgroups

$$Z(1) = Z_1 + Z_2 + \cdots + Z_i + \cdots + Z_n \qquad (15)$$

where Z_1, given by Eq. 13, counts all chain conformations with segment 1 in layer 1, Z_2 counts all chain conformations with: 1) segment 2 in layer 1 and 2) segment 1 not in layer 1. There are no conditions on segments 3 to n (except connectivity). Condition (2) excludes from Z_2 conformations already counted in Z_1, namely those with both segments 1 and 2 in layer 1. Z_3 counts conformations with 1) segment 3 in layer 1 and 2) segments 1 and 2 not in layer 1, but with no restrictions on segments 4 to n, etc.

In this way we consider for each term Z_i in Eq. 15 two subchains, the front part consisting of segments 1 to $i - 1$, and the back part consisting of segments i to n. The back part may have all conformations of an $n - i + 1$ segment chain with its first segment in layer 1. Following Eq. 13 this number is

$$Z'_{n-i+1} = [e^{\phi_1}\ 0 \cdots 0]G_{n-i+1}^{n-i}\, u_{n-i+1} \qquad (16)$$

where, as in Eq. 13, the subscripts of G and of u indicate the size of the matrix or vector. Each of the conformations in Eq. 16 may be combined with any one of the conformations of the front part of the chain:

$$Z_i = Z^*_{i-1}Z'_{n-i+1} \qquad (17)$$

We now formulate Z^*_{i-1} for the $i - 1$ segment subchain with the condition that none of its segments is in the first layer. Because the subchain is connected to segment i in layer 1, segment $i - 1$ must be in layer 2 and has, therefore, the distribution vector

$$\nu_{i-1} = \left[\frac{r_2}{r_1}e^{\phi_2}\ 0 \cdots 0\right] \qquad (18)$$

Mathematically, it is most convenient to compute the partition function by working backward from segment $i - 1$ in layer 2 to chain segment 1 in some outer layer. Hence, given v_{i-1} by Eq. 18, the desired partition function is generated by

$$Z_{i-1}^* = v_{i-1}\, \mathbf{G}_{i-1}^{*\,i-2}\, \mathbf{u}_{i-1} \tag{19}$$

provided that the matrix $\mathbf{G}_{i-1}^*$ propagates the chain only in layers 2 to i, but not into or out of layer 1. This $(i - 1) \times (i - 1)$ matrix is formed from the $i \times i$ matrix $\mathbf{G}_i$, Eq. 10, by eliminating the first column and the first row:

$$\mathbf{G}_{i-1}^* = \begin{bmatrix} (z_c - 2)e^{\phi_2} & \dfrac{r_3}{r_2}e^{\phi_3} & 0 & \cdot \\[2ex] \dfrac{r_2}{r_3}e^{\phi_2} & (z_c - 2)e^{\phi_3} & \dfrac{r_4}{r_3}e^{\phi_4} & \cdot \\[2ex] 0 & \dfrac{r_3}{r_4}e^{\phi_3} & (z_c - 2)e^{\phi_4} & \cdot \\[2ex] \cdot & \cdot & \cdot & \cdot \end{bmatrix} \tag{20}$$

Equations 15–19 now yield the total number of conformations of an n segment chain having at least one of its segments in layer 1

$$Z(1) = \sum_{i=1}^{n} \left\{ \left[\dfrac{r_2}{r_1}e^{\phi_2}\, 0 \cdots 0 \right] \mathbf{G}_{i-1}^{*\,i-2}\mathbf{u}_{i-1} \right\} \tag{21}$$

$$\cdot \{[e^{\phi_1} 0 \cdots 0]\mathbf{G}_{n-i+1}^{n-i}\mathbf{u}_{n-i+1}\}$$

We then compute the number $Z(2)$ of chain configurations without any segment in layer 1, but at least one segment in layer 2. We use the same method as for $Z(1)$. The result is the same as Eq. 21 but with e^{ϕ_1} replaced by e^{ϕ_2}, $r_2/r_1e^{\phi_2}$ by $r_3/r_2e^{\phi_3}$, $\mathbf{G}$ by $\mathbf{G}^*$, and $\mathbf{G}^*$ by the matrix $\mathbf{G}^{**}$ obtained from $\mathbf{G}$ by eliminating columns 1 and 2 and rows 1 and 2. In the same way $Z(j)$ can be derived from $Z(j - 1)$. We compute successive terms in the converging series for the excess number of conformations bound in successive layers with the sum

$$Z_{\text{bound}} = \sum_{j=1}^{\infty} [Z(j) - Z_{\text{bulk}}] \tag{22}$$

We now compute the binding constants, K_{obs}, from this partition function. In the bulk solution, at potential $\phi = 0$, a ligand with n segments may assume z_c^{n-1} different conformations:

$$Z_{\text{bulk}} = z_c^{n-1} \tag{23}$$

The binding free energy of ligands in layer j is with Eq. 22

$$\Delta f_j = kT \ln \dfrac{Z(j) - Z_{\text{bulk}}}{Z_{\text{bulk}}} \tag{24}$$

Exponentiating and multiplying by the bulk ligand concentration $[L]$, the excess concentration of ligand bound in layer j is

$$[L]e^{\Delta f_j /kT} = [L]\dfrac{Z(j) - Z_{\text{bulk}}}{Z_{\text{bulk}}} \tag{25}$$

To derive K_{obs} we proceed as in Eqs. 5 to 7, but replacing the integration in Eq. 6 by a summation over the lattice cross section. The result is

$$K_{\text{obs}} = N_{\text{av}}10^{-27}\text{b} \sum_{j} \dfrac{Z(j) - Z_{\text{bulk}}}{Z_{\text{bulk}}}A_j \tag{26}$$

where A_j is the cross-sectional area of lattice layer j, see Fig. 4,

$$A_j = \pi\,[(a + jc)^2 - (a + (j - 1)c)^2] \tag{27}$$

In all cases treated in this report we find that Z_{bulk} may be neglected compared to $Z(j)$. Furthermore, terms with $j > 1$ do not contribute significantly in Eqs. 22 and 26. In other words, only binding in the first layer is significant. Therefore, good approximations of Eqs. 22 and 26 are

$$Z_{\text{bound}} \approx Z(1) \tag{28}$$

and

$$K_{\text{obs}} \approx N_{\text{av}}10^{-27}b\,\dfrac{Z(1)}{Z_{\text{bulk}}}\,\pi[(a + c)^2 - a^2] \tag{29}$$

It is customary (Mascotti and Lohman, 1992, 1993) to derive a molar binding free energy from the expression:

$$G_{\text{obs}} = -RT\ln K_{\text{obs}} \tag{30}$$

The temperature dependence of G_{obs} gives the enthalpy and entropy of binding, H_{obs} and S_{obs}, respectively.

$$H_{\text{obs}} = \dfrac{\partial(G_{\text{obs}}/T)}{\partial(1/T)} \quad \text{at constant salt concentration} \tag{31}$$

$$TS_{\text{obs}} = -G_{\text{obs}} + H_{\text{obs}} \tag{32}$$

COMPARISON WITH EXPERIMENTS

We compare the theory against several sets of experimental data involving various ligands binding to three types of polyions: B-DNA, single stranded polynucleotides, and heparin. Our models depend on two parameters: the radius a of the cylinder and the axial distance b between the fixed charges. For B-DNA we take $a = 10$ Å, from the known distance between the phosphate charges and the helical axis, and $b = 1.685$ Å, from the known axial distance between phosphate charges. These are structural dimensions; we compare results obtained using those values to results obtained using dimensions from kinetic experiments (Schellman and Stigter, 1977). Diffusion and intrinsic viscosity of B-DNA are consistent with a shear surface at $a = 12$ Å; electrophoresis of B-DNA in NaCl solutions indicates that

about 27 percent of the Na^+ counterions are inside the shear surface, giving $b = 1.685/0.73 = 2.308$ Å. Because of the simplicity of the model, it is not clear which set of parameters is better justified, so we use both sets of parameters in the theory to determine the sensitivity of the theory to them. Next, using B-DNA as a model, we assume $a = 7$ Å and $b = 3.37$ Å for single stranded polynucleotides and compare also with the parameter set $a = 6$ Å and $b = 4$ Å. Heparin is a sulfated polysaccharide, for which we use $a = 6$ Å and one negative charge per $b = 2.9$-Å rod length, based on data cited by Mascotti and Lohman (1995).

Binding of Mg^{2+} to polynucleotides

The binding of Mg^{2+} to poly(A), poly(U) and their complexes was measured by Krakauer (1971, 1974), and reinterpreted by Record et al. (1976). In the presence of 0.029M Na^+, Eq. 7 with $z = 2$ gives $\log K_{obs} = 2.61$ although the experiments show $\log K_{obs} = 2.9 \pm 0.1$ to 3.7 ± 0.1. For the slopes, theory predicts $\partial \log K_{obs}/\partial \log M_{salt} = -1.72$ in comparison to experimental values of $\partial \log K_{obs}/\partial \log M_{salt} = -1.2 \pm 0.1$ to -1.7 ± 0.1, depending on the polynucleotide. These predictions are in reasonable agreement with the experiments.

Binding of $Co(NH_3)_6^{3+}$ to B-DNA

Fig. 5 compares Eq. 7 with experiments for the binding of $Co(NH_3)_6^{3+}$ to calf thymus DNA by Plum and Bloomfield

(1988). The experimental binding constants are closer to the predictions with the kinetic than with the structural parameters. This may be due to the large size of the $Co(NH_3)_6^{3+}$ ions because the fraction of counterions inside the shear surface of B-DNA decreases with increasing counterion size (Schellman and Stigter, 1977). The salt dependence of binding in Fig. 5 is predicted by either set of DNA parameters: The theoretical curves in Fig. 5 are nearly straight lines, with average slopes -2.69 for the dashed curve and -2.39 for the solid curve.

Binding of oligolysines to polynucleotides

Figs. 6 and 7 compare the theory with the experiments of Mascotti and Lohman (1990). We found that without the lattice modeling of the chain entropies, the slopes of the binding constant with salt were given correctly by Eq. 7, but the absolute binding constants (not shown) were too high: for the $z = 10$ ligand the error was more than a factor of 1000. Fig. 6 shows the full theory, including the chain entropy, which is much better, but the theory now somewhat underestimates the experimental binding constants. One possible source of this error is the simplification introduced by our use of a lattice cell size of $c = 6.2$ Å, which implies that the ligand charges placed at the cell centers in layer 1 are $a + c/2 = 10.1$ Å from the rod axis. It is likely that lysine charges may approach poly(U) more closely than this. We then chose to allow the charge placement within the lattice cells to be an adjustable parameter, because the lattice itself is an arbitrary construct. When the ligand
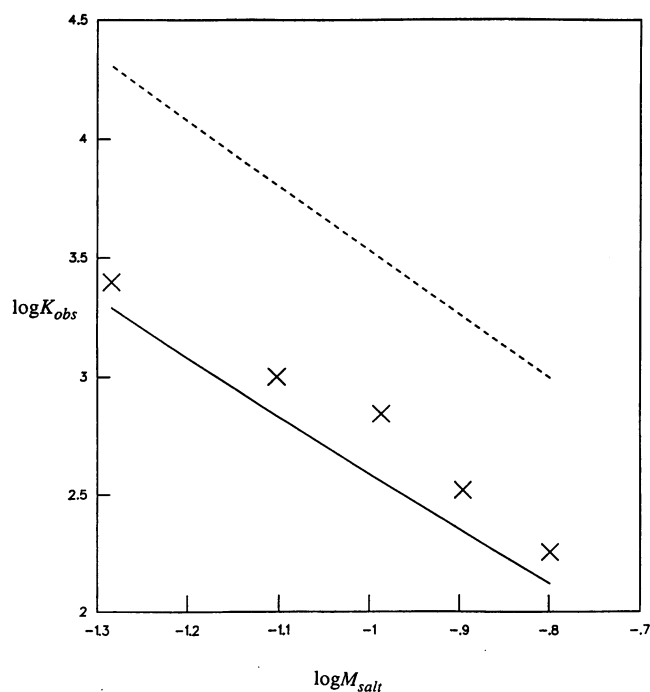

FIGURE 5 Binding constants of $Co(NH_3)_6^{3+}$ to B-DNA versus monovalent salt concentration. Crosses: experiments by Plum and Bloomfield (1988) on binding to calf thymus DNA. Full curve, theory from Eq. 7 for kinetic model of B-DNA. Dashed curve, theory from Eq. 7 for structural model of B-DNA.
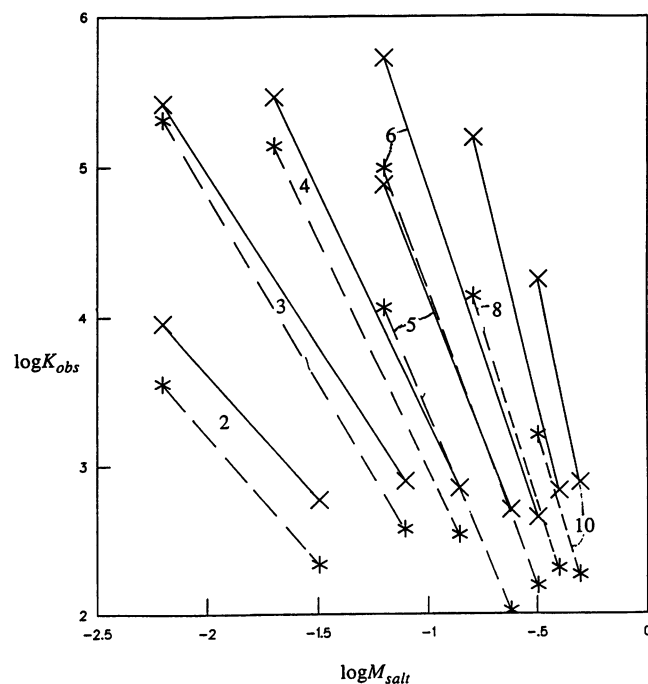

FIGURE 6 Binding constants of oligolysines to poly(U) versus monovalent salt concentration. Full lines, experimental data from Fig. 2. Dashed lines, theory from Eq. 14 and Table 2 with ligand charges in cell centers.
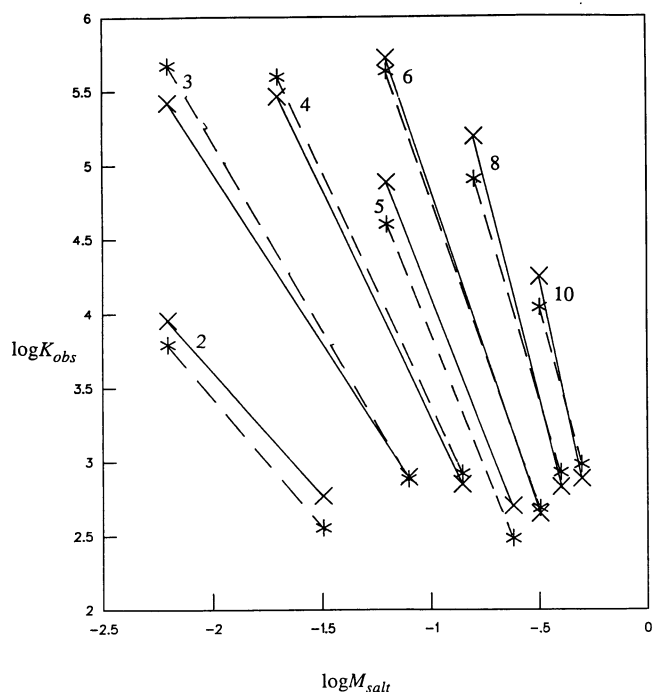
FIGURE 7   As for Fig. 6, but with ligand charges shifted 0.8 Å inward.

FIGURE 8   Thermodynamic functions versus monovalent salt concentration for binding of pentalysine to poly(A) and to poly(U) at 25°C. From top down data for entropy TS_b, for enthalpy H_b, and for free energy G_b. Dashed lines, experiments by Mascotti and Lohman (1992, 1993) for binding to poly(A) (*) and to poly(U) (O). Solid lines, theory for model of Fig. 7.

charges are placed 0.8 Å further inward from the cell center, Fig. 7 shows that the theory predicts well the absolute binding constants to poly(U).

The predicted slopes of K_{obs} with salt, from the dashed lines in Fig. 7, are given in the last column of Table 1. The agreement with the Mascotti and Lohman data is within experimental scatter, except for $z = 8$ and 10 where the high salt concentration probably makes the PB equation less reliable.

Although the free energies are well predicted by the theory, Fig. 8 shows that the enthalpy and entropy for pentalysine binding to poly(A) are also well predicted, but not so accurately for binding to poly(U). The solid curves are predictions from Eqs. 30–32, assuming that the ligand charges are located 0.8 Å inward from the cell centers, as in Fig. 7 above. Part of the discrepancy is due to the large uncertainty of the experimental values derived from the dependence of K_{obs} on temperature, about 1.5 kcal/mol for both H_b and TS_b.

The theoretical results do not depend strongly on the parameters of the polynucleotide model. Changing the cylinder radius and the axial charge distance from $a = 7$ Å and $b = 3.37$ Å to $a = 6$ Å and $b = 4$ Å does not influence the fit with experiments in Figs. 7 and 8 significantly, provided that the lysine charges are placed 1.0 Å, instead of 0.8 Å, inward from the cell center.

Detailed analysis of the various contributions to the partition function reveals that the bound lysine residues mainly occupy sites in the first lattice layer. This shows that the dominant structures of bound oligolysines are wrapped around the poly(U) strand or at least closely held by it.
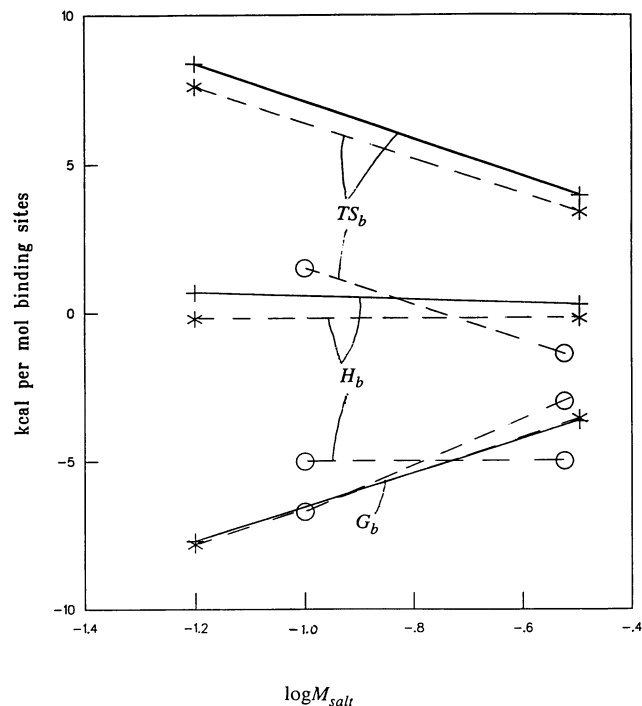
Polyamine binding to DNA

By equilibrium dialysis, Braunlin et al. (1982) have studied the binding to T7 DNA of the following polyamines: spermine, $NH_2-(CH_2)_3-NH-(CH_2)_4-NH-(CH_2)_3-NH_2$; spermidine, $NH_2-(CH_2)_3-NH-(CH_2)_4-NH_2$; putrescine, $NH_2-(CH_2)_4-NH_2$.

The experiments were carried out at pH 6.5 and with various NaCl concentrations. We compare with the structural model of B-DNA, i.e., using $a = 10$ Å and $b = 1.685$ Å. We divide the amines into charged segments and assign one charged segment to a cell, with $n = 4$ for spermine, $n = 3$ for spermidine, and $n = 2$ for putrescine, assuming a cubic cell size of $c = 4.37$ Å. In Fig. 9 Eq. 29 for delocalized binding, with the ligand charges in the cell centers, is compared with experiments by Braunlin et al. (1982). The slopes are predicted within experimental error. The predictions of K_{obs} for spermine and spermidine are very good, but low for putrescine.

Binding of tripeptides to heparin

We consider the experiments by Mascotti and Lohman (1995) on the binding to heparin of L-lysyl-L-tryptophanyl-L-lysine carboxylate ($KWK - CO_2 = K^{2+}WK^{+}$) and L-arginyl-L-tryptophanyl-L-arginine carboxylate ($RWR-CO_2 = R^{2+}WR^{\pm}$). The ligand binding was monitored through spectral change of the tryptophan residue. Therefore, the
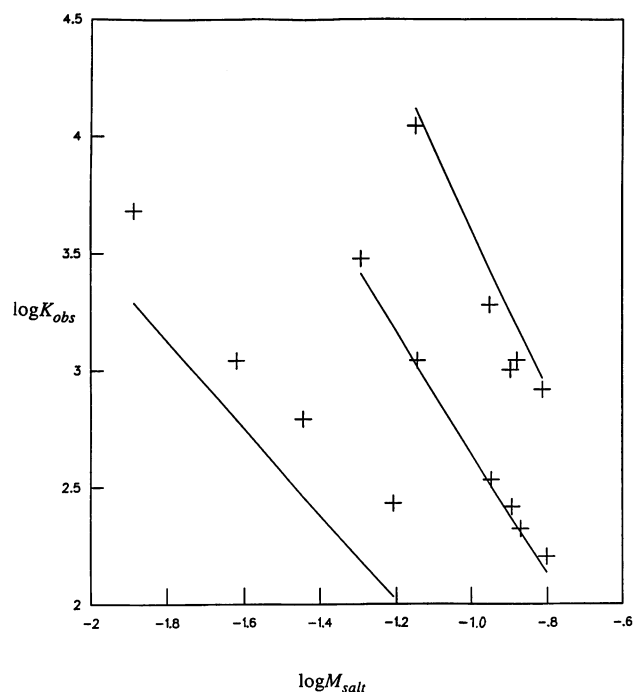
FIGURE 9 Binding constants of polyamines to T7 DNA. From left to right putrescine, spermidine, spermine. Crosses, experiments by Braunlin et al. (1982). Theory for structural model of B-DNA. Solid curves, theory from Eq. 29 with ligand charges in cell centers.

FIGURE 10 Binding constant of tripeptides to heparin versus monovalent salt concentration, with asterisks for $KWK-CO_2$ and crosses for $RWR-CO_2$. Dashed curves, experiments by Mascotti and Lohman (1995). Solid curves, theory from Eq. 14 and Table 2 with $\theta = 1.8\ kT$ for $KWK-CO_2$ and $\theta = 2.1\ kT$ for $RWR-CO_2$.

theory is formally the same as developed for the localized binding of oligolysines to polynucleotides in Eq. 14 and Table 2, with $z = 2$ and $n = 3$ in this case. As before we take a pseudocubic lattice with coordination number $z_c = 6$ and layer thickness $c = 6.2$ Å, and put the peptide charges 0.8 Å inward from the cell centers, as in Fig. 7 for the binding of oligolysines. Because there is no experimental information on the adsorption potential of tryptophan to heparin we choose a value for θ in Eq. 14 that gives the best agreement with experiment.

In Fig. 10 theoretical binding constants are compared with experimental values. Agreement within experimental error is obtained with $\theta = 1.8kT$ for $K^{2+}WK^{\pm}$ and with $\theta = 2.1kT$ for $R^{2+}WR^{\pm}$. Figs. 11 and 12 compare thermodynamic data derived from binding constants and their temperature dependence, using in the model computations the same θ values as in Fig. 10. For binding of the lysine peptide to heparin in Fig. 11 the agreement between theory and experiment is within experimental errors which are 1.5 kcal/mol for H_b and TS_b. For binding of the arginine peptide in Fig. 12 the discrepancies between theory and experiment are well outside the experimental uncertainties of H_b and TS_b. In agreement with the suggestion of Mascotti and Lohman (1995), we find that arginine binds to heparin with greater affinity than lysine.

DISCUSSION

What is the physical basis for binding? Record et al. (1976) have said that counterion release is "...the dominant factor
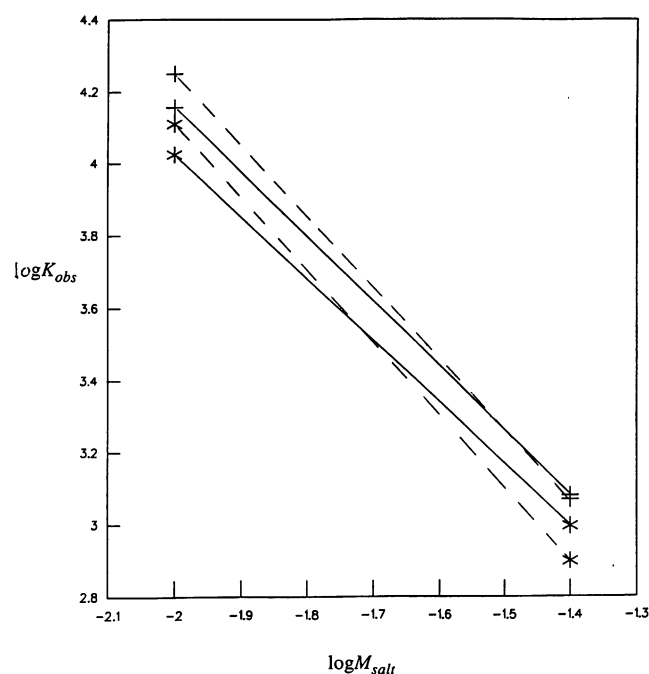
driving complex formation between these charged ligands and the nucleic acid..." That is, because electroneutrality must be preserved, Record et al. (1976) recognized that there is an ion exchange process: upon binding of a ligand ion L^{z+} the polyion must release counterions with total charge z^+ from its ionic atmosphere to the bulk salt solution. This assumes that ligand binding does not perturb the distribution of coions. However, although counterion release describes the result of the electroneutrality constraint, it is not a good description of the driving force, which we regard as being the electrostatic attraction between polyelectrolyte and ionic ligand.

One puzzle about the binding of ionic ligands to polyelectrolytes is why the binding isotherm is so well described by the theory of McGhee and von Hippel (1974) for the adsorption of ligands that, except for excluded volume, do not interact. That is, two ions bind to the polyion as if they were independent, rather than repulsive. We believe this arises because the binding of each ion is an electroneutral displacement, so the ion atmosphere of the polyion is not altered by the binding of each ion.

According to our theory, conformational entropy opposes the binding of chain ligands, leading to binding constants around $10^4 - 10^5$ (see Fig. 7). Good tight-binding drugs such as DAPI, Hoechst 33258, Netropsin (Misra et al., 1994a,b) have binding constants 3 to 4 orders of magnitude higher than this, perhaps because they are more rigid or have more specific interactions than we have treated here.
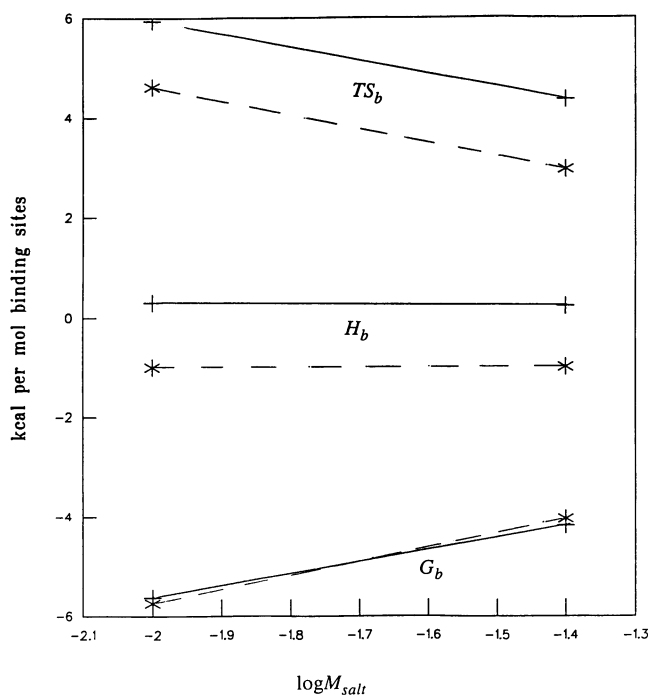
FIGURE 11   Thermodynamic functions versus monovalent salt concentration for binding of $KWK-CO_2$ to heparin at 25°C. From top down data for entropy TS_b, for enthalpy H_b, and for free energy G_b. Dashed lines, experiments by Mascotti and Lohman (1995). Solid lines, theory for model of Fig. 10.

FIGURE 12   Same as Fig. 11, but for $RWR-CO_2$.

Our theory has the following limitations. First, we are using the PB theory which is approximate, and does not handle multivalent counter ions well. It has been found that for properties most dependent on the "far" field behavior distant from the charged rod, results in monovalent salt solutions may not be particularly sensitive to flaws of the model. For example, predictions by the PB theory of the electrostatic repulsion between straight rods of B-DNA in monovalent salt solutions (Stigter, 1977, 1987) are in excellent agreement with experiments on pair repulsions between short sections of DNA in 1) sedimentation (Brian et al., 1981), 2) light scattering (Nicolai and Mandel, 1989; Fixman, 1990; Stigter and Dill, 1993), and 3) probabilities of knot formation in coiled DNA (Vologodskii and Cozzarelli, 1994). However, ionic binding to polyelectrolytes depends on attractive interactions whose short range makes them much more sensitive to details of the model. Specific interactions might become significant, and the geometric fit of oligolysine ligands and polynucleotide might affect the binding constant. Errors might also arise from our assumption that the potential field ψ depends only on the radial distance from the rod, and not on angular positions around the rod. Some of these uncertainties are probably reflected in the adjustable parameter of the binding theory: the distance of closest approach between ligand charge and polyelectrolyte. Experiments by Mascotti and Lohman (1993) show that binding of oligolysines depends significantly on the type of polynucleotide.
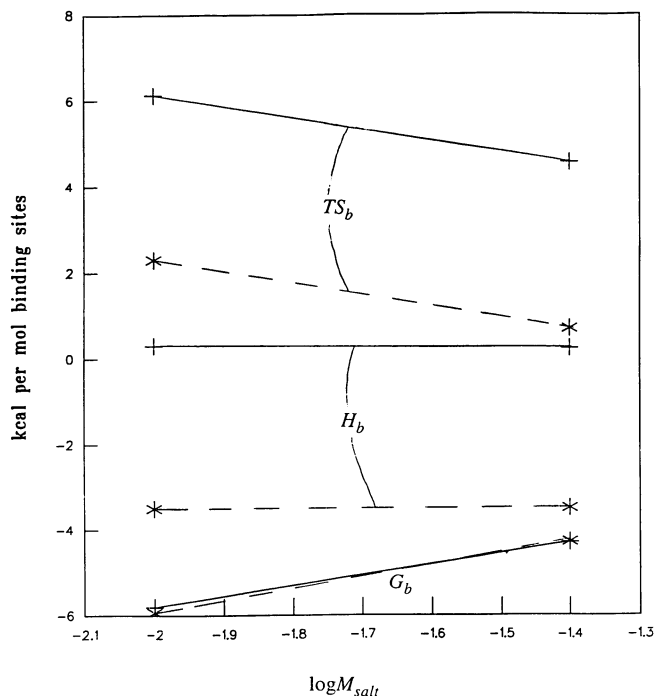
CONCLUSIONS

We have presented a simple theory for the binding of ionic ligands to polyelectrolytes modeled as charged rods. It is based on the use of the Poisson-Boltzmann theory for the electrostatic potential around charged rods. The dilute ligand binding is affected by the electrostatics of the rod surrounding by its electrolyte solution. When the ligand itself is a chain, having some flexibility, we account for the conformational changes on binding using a lattice model for chains near surfaces. This model is very simple because it does not incorporate the structural details that are included in finite difference PB methods; nevertheless it works remarkably well. For small rigid molecules binding to polyions, the theory predicts well the slope of binding constant with salt, and the absolute binding constants themselves, without adjustable parameters. For flexible ligands, free energies are also in good agreement with experiment, provided we use the distance of closest approach of the ligand to the rod as the one adjustable parameter. Some enthalpies and entropies of binding are given well by the theory, but others are not.

REFERENCES

Anderson, C. F., and M. T. Record, Jr. 1982. Polyelectrolyte theories and their applications to DNA. *Annu. Rev. Phys. Chem.* 33:191–222.

Anderson, C. F., and M. T. Record, Jr. 1993. Salt dependence of oligoion-polyion binding: a thermodynamic description based on preferential interaction coefficients. *J. Phys. Chem.* 97:7116–7126.

Braunlin, W. H., T. J. Strick, and M. T. Record, Jr. 1982. Equilibrium dialysis studies of polyamine binding to DNA. *Biopolymers.* 21: 1301–1314.

Brian, A. A., H. L. Frisch, and L. S. Lerman. 1981. Thermodynamics and equilibrium sedimentation analysis of the close approach of DNA molecules and a molecular ordering transition. *Biopolymers.* 20:1305–1328.

Dill, K. A., J. Naghizadeh, and J. A. Marquesee. 1988. Chain molecules at high densities at interfaces. *Annu. Rev. Phys. Chem.* 39:425–461.

Fixman, M. 1990. Polyelectrolyte bead model. I. Equilibrium. *J. Chem. Phys.* 92:6283–6293.

Friedman, R. A. G., and G. S. Manning. 1984. Polyelectrolyte effects on site-binding equilibria with applications to the intercalation of drugs into DNA. *Biopolymers.* 23:2671–2714.

Hill, T. L. 1958. Osmotic pressure, protein solutions and active transport. II. *J. Am. Chem. Soc.* 80:2923–2926.

Krakauer, H. 1971. The binding of Mg^{++} ions to polyadenylate, polyuridylate, and their complexes. *Biopolymers.* 10:2459–2490.

Krakauer, H. 1974. A thermodynamic analysis of the influence of simple mono- and divalent cations on the conformational transitions of polynucleotide complexes. *Biochemistry.* 13:2579–2589.

Latt, S. A., and H. A. Sober. 1967a. Protein-nucleic acid interactions. II. Oligopeptide-polyribonucleotide binding studies. *Biochemistry.* 6:3293–3306.

Latt, S. A., and H. A. Sober. 1967b. Protein-nucleic acid interactions. III. Cation effect on binding strength and specificity. *Biochemistry.* 6:3307–3314.

Manning, G. S. 1978. The molecular theory of polyelectrolyte solutions with applications to the electrostatic properties of polynucleotides. *Q. Rev. Biophys.* 11:179–246.

Mascotti, D. P., and T. M. Lohman. 1990. Thermodynamic extent of counterion release upon binding oligolysines to single-stranded nucleic acids. *Proc. Natl. Acad. Sci. U. S. A.* 87:3142–3146.

Mascotti, D. P., and T. M. Lohman. 1992. Thermodynamics of single-stranded RNA binding to oligolysines containing tryptophan. *Biochemistry.* 31:8932–8946.

Mascotti, D. P., and T. M. Lohman. 1993. Thermodynamics of single-stranded RNA and DNA interactions containing tryptophan. Effects of base composition. *Biochemistry.* 32:10568–10579.

Mascotti, D. P., and T. M. Lohman. 1995. Thermodynamics of charged oligopeptide-heparin interactions. *Biochemistry.* 34:2908–2915.

McGhee, J. D., and P. H. J. von Hippel. 1974. Theoretical aspects of DNA-protein interactions: co-operative and non-co-operative binding of large ligands to a one-dimensional homogeneous lattice. *J. Mol. Biol.* 86:469–489.

McMillan, W. G., and J. E. Mayer. 1945. The statistical thermodynamics of multicomponent systems. *J. Chem. Phys.* 13:276–305.

Misra, V. K., J. L. Hecht, K. A. Sharp, R. A. Friedman, and B. Honig. 1994a. Salt effect on protein-DNA interactions: the λcI repressor and EcoRI endonuclease. *J. Mol. Biol.* 238:264–280.

Misra, V. K., K. A. Sharp, R. A. Friedman, and B. Honig. 1994b. Salt effect on ligand-DNA binding: minor groove binding antibiotics. *J. Mol. Biol.* 238:245–263.

Nicolai, T., and M. Mandel. 1989. Ionic strength dependence of the second virial coefficient of low molar mass DNA fragments in aqueous solutions. *Macromolecules.* 22:438–444.

Plum, G. E., and V. A. Bloomfield. 1988. Equilibrium dialysis study of binding of hexammine cobalt(III) to DNA. *Biopolymers.* 27:1045–1051.

Record, M. T., Jr., T. M. Lohman, and P. J. de Haseth. 1976. Ion effects on ligand-nucleic acid interactions. *Mol. Biol.* 107:145–158.

Riggs, A., H. Suzuki, and S. Bourgeois. 1970a. lac repressor-operator interaction I. Equilibrium studies. *J. Mol. Biol.* 48:67–83.

Riggs, A., S. Bourgeois, and M. Cohn. 1970b. The lac repressor-operator interaction III. Kinetic studies. *J. Mol. Biol.* 53:401–415.

Rubin, R. J. 1965. Random-walk model of chain-polymer adsorption at a surface. *J. Chem. Phys.* 43:2392–2407.

Schellman, J. A., and D. Stigter. 1977. Electrical double layer, zeta potential, and electrophoretic charge of double-stranded DNA. *Biopolymers.* 16:1415–1434.

Stigter, D., and T. L. Hill. 1959. Theory of the Donnan membrane equilibrium. II. Calculation of the osmotic pressure and of the salt distribution in a Donnan system with highly charged colloid particles. *J. Phys. Chem.* 63:551–556.

Stigter, D. 1975. The charged colloidal cylinder with a Gouy double layer. *Colloid Interf. Sci.* 53:296–306.

Stigter, D. 1977. Interactions of highly charged colloidal cylinders with applications to double-stranded DNA. *Bipolymers.* 16:1435–1448.

Stigter, D. 1987. Donnan membrane equilibrium, sedimentation equilibrium, and coil expansion of DNA in salt solutions. *Cell Biophys.* 11: 139–158.

Stigter, D., and K. A. Dill. 1993. Theory for second virial coefficient of short DNA. *J. Phys. Chem.* 97:12995–12997.

Stigter, D. 1995. Evaluation of the counterion condensation theory of polyelectrolytes. *Biophys. J.* 69:380–388.

Vologodskii, A. V., and N. R. Cozzarelli. 1994. Conformational and thermodynamic properties of supercoiled DNA. *Annu. Rev. Biophys. Biomol. Struct.* 23:609–643.

Wilson, R. W., D. C. Rau, and V. A. Bloomfield. 1980. Comparison of polyelectrolyte theories of the binding of cations to DNA. *Biophys. J.* 30:317–326.